International Journal of Engineering & Technology, 7 (3.2) (2018) 141-148

International Journal of Engineering & Technology

Website: www.sciencepubco.com/index.php/IJET

Research paper

The Problem of Consideration Torsion Emergence in Beams

Sergiy Hudz[1]*, Grygorii Gasii[2], Volodymyr Pents[3]

[1]Poltava National Technical Yuri Kondratyuk University, Ukraine
[2]Poltava National Technical Yuri Kondratyuk University, Ukraine
[3]Poltava National Technical Yuri Kondratyuk University, Ukraine
**Corresponding Author E-Mail: Goods.Sergiy@Gmail.Com*

Abstract

The calculation of the steel unrestrained and partially restrained roof beams with initial imperfections main stages is discussed. Restraining can be done by structures attached to the steel beams, namely, profiled flooring and discrete joints. On the basis of the new approach to the internal forces analysis and the geometric properties specification, the purpose was to find and describe the differences in the beam work as the part of roofing, which distinguishes it from the work conditions of the free supported beam. The features of the beam operation with the joint flexural and torsion are singled out. The need to improve the existing theoretical model for present deficiencies elimination is indicated. The bearing capacity determining methods for the flexible elements stability exposed to bending and bending with torsion are compared. Their advantages and disadvantages are revealed. It is proposed to increase the material saving by applying calculations. At the end of the article, conclusions regarding the consideration of investigated factors are given.

Keywords: *bimoment; critical load; lateral-torsional buckling; restraint; steel beam; torsion; warping stresses.*

1. Introduction

In steel beams with different functions and open cross-sections, their stress caused by the presence of warping torsion deformation may occur due to the load eccentric application. The problem of consideration these stresses is closely related to the phenomenon of flexural-torsional buckling, which is called "lateral-torsional buckling" (LTB) for beams. It is necessary to pay attention to the existing contradiction, which consists in the discrepancy among the partially restrained construction performance of most classical theoretical ideas about the thin-walled rods warped torsion. Mathematical models, as a rule, consider not all the peculiarities of the structural behavior as a part of the roof, especially with the significant stiffness of the attached elements. In such cases, the simulation often has little in common with the actual processes, does not correspond to the real picture of the stress-strain state and needs to be clarified for adequate mapping the stress cross-sectional use degree needed to ensure the structure reliability in general. In order to increase the calculation accuracy and to keep it close to the structure work actual conditions, internal forces need to be determined according to the nonlinear theory of the second order. It considers geometric nonlinearity and represents the deformed scheme calculation where the equation of equilibrium is registered for the system deformed state.
Unsolved earlier part of the general problem is the allocation of the features that need to be considered when calculating insufficiently restrained beams to match the constructed model with the actual work of beams at complex resistance. Purpose and objectives of research were to study the torsion physical origin, causes and effects of torsion emergence and the ways to control or avoid it.

2. The main body

2.1 Analysis of Recent Sources of Research and Publications

Modern theoretical and experimental-theoretical studies of the stress-strain state and stability of thin-walled steel beams, without restraining and restrained, are presented in [1, 2, 3] and other researchers. Among the main sources, where the results of beam torsion and stability research are noted, the works of the German classical technical school representatives are included [4, 5, 6]. The theoretical foundations of the thin-walled roads theory are presented in the papers of the Soviet classical school scientists [7, 8]. The I-beam work under the action of bending moment and bimoment is considered in the article [9], but these studies do not consider the influence of the torsion angle on the bending moments. Experimental studies of steel I-beam work with the joint action of flexural and torsion were conducted under Tusnin A.R. [10]. In the paper [11] it is experimentally confirmed that the deformation of the contour at torsion even for some cold-formed profiles can be neglected. The application of the energy method to stability problems has been rapidly developing at present and is accompanied by the implementation of computerized computational methods [12, 13]. The behavior and calculation of steel structures in accordance with European norms EN 1993 are described in the manuals [14, 15]. The concept of the LTB theory is contained in the source [16]. The calculation of equivalent loads for stabilizing structures is given and analyzed in the dissertation [17]. One of the authors of this article investigated this issue in [18, 19].

2.2 Causes of Torsion Emergence in Beams

The straight I-beam flexed in the web may break down due to the loss of its general stability. When the load reaches the critical value, such a beam starts to buckle and exit the bending plane (Fig. 1).

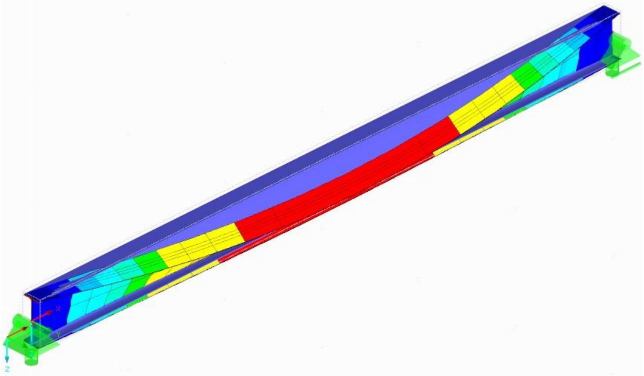

Fig. 1: Exit of an unrestrained beam from the bending plane by LTB

But the most frequent torsion occurs at the beginning of construction loading. This happens in the following cases:
- off-center application of the load (for example, in the case of one-sided loading during installation, at different loads on both sides);
- the transverse bending of the beam in two planes (in the case when the beam serves as a purlin of a sloping roof or transverse frame girder, which perceives the horizontal load from the wind in the level of the upper flange);
- the presence of initial geometric imperfections of the beam arising from the accidental formation of defect, damage, or from a purposeful change in the object shape (the curvature of the beam axis in the plane of least stiffness, cross-section pre-torsion);
- channel girders and other beams with asymmetric cross-section application.

Despite such circumstances of the structure work, for example, steel purlins of the sloping roof are usually calculated as split beams under the action of uniformly distributed along the whole span on the skew bending without considering torsion. Under the action of bending moments in two main planes, the algebraic sum of the design ratios according to the normal stresses of each one is determined and compared with the unity. This is valid only if the hypothesis of plane cross-sections is adopted. When torsion, the plane of the cross-section is broken and there are additional stresses and deformations, called the cross-section distortion. Numerous theoretical and practical studies have shown that the cross-section distortion influences normal stresses more than shearing ones. This influence is considered by the introduction of an additional component of the stresses upon bimoment action, namely warping stresses. Negative stresses values may also be extreme, so the unity requires comparing with the algebraic sum absolute value.

To verify the stability of the beam bending in the web, it was decided to determine the stresses in the compressed flange and compare them with critical ones, which were equal to the yield strength multiplied by the reduction factor for LTB, which depends on the design model, the geometric properties of the cross-section and the distance between the fastening points of compressed beam flange. The formulas that determine this factor were derived without possible eccentricities of load application for the ideal elastic beam, which ends have hinged support and free are distorted, and the influence of the real beam geometric imperfections in the form of initial curvatures is calculated mainly with the introduction of additional constant coefficient.

When transferring the load through the sufficiently rigid floor, which continuously is supported with compressed flange and reliably is jointed with it, as well as compliance with requirements in ratio of geometric dimensions, checking the stability of I-beam cross-section bending in the web plane or in two planes, usually is not executed. When flat or profiled metal decking is used, it is sometimes unreasonably considered to be reliable to connect them with beam compressed flange by welding, on bolts or self-tapping screws, observing constructive requirements for joining. In other cases, with the insufficient fastening of the compressed flange, it is necessary to perform the beam stability calculation according to the formula with reduction factor for LTB. When determining it, it is advisable to consider the rotational or rotational and shear stiffness of the structures, which discretely or continually restrain the compressed flange of the beam in most of the cases and reduce the deformation of its displacement. It can be done according to [4, 5, 6] or in the popular LTBeam computer program.

While the joint action of bending and torsion, buckling is developed reaching critical load, where the beam bearing capacity is exhausted. On the level of beam normal stresses, in addition to the load, such factors such as beam span, cross-section angle of slope, shear and rotational stiffness of profiled flooring, form and geometric properties of the beam cross-section, the beam curvature size and the steel yield influence.

In order to determine the relative slenderness, which influences the reduction factor for LTB, it is necessary to know the elastic critical moment for LTB. The value of M_{cr} for the hinged-on ends of the I-beam loaded with a uniformly distributed load can be set according to the National Application Document to EN 1993-1-1. In other cases, it is advisable to quantify the critical moment using simulation. For the hinged beam supported at the ends which is loaded with uniformly distributed load and support bending moments, there is the method for determining the critical moment M_{cr}, which is given in manual [14] or in p. 6.6 of [4] and developed in the NCCI SN003a, where under these conditions and under different boundary conditions and the load types, the value of the coefficients is shown in the graphs, and also the use of the LTBeam program is recommended.

The inclination of the beam to instability arises due to insufficient restraint of the compressed flanges of the beam with attached structures, includes: monolithic and prefabricated reinforced concrete slabs; steel flat and bearing profiled flooring, sandwich panels and other enclosing structures; purlins, floor beams and other minor beams; discrete ligaments (horizontal cross joints, ropes). The first two types of structures can be attributed to the continual joints, the other two belong to the discrete ones. These structures reduce the effective length of the beam and increase its overall stability. The combination of steel rod elements with reinforced concrete planes leads to the formation of space composite structures, which have acquired useful properties. Their efficiency has already been proved earlier [20]. Lightweight roofs consist of purlins that can be based on the main beams (frame girders) on top or adjacent to them at one level, and the flooring of the steel profiled sheet, which stiffness is used to increase the stability and fastening beams from torsion. Also, additional stabilization of beams can occur due to measures for the installation of structural components: flat and volume stiffness ribs, downstands in the supporting areas and the adjacency of the columns in the areas of support.

2.3 Stress, Strain and Internal Forces in the Cross-Section of the Steel Beam

Flexible, thin-walled beams perceive, in addition to bending stresses, also torsion stress. To find the maximum total normal stresses $\sigma_{\max}$, considering torsion, it is possible to simplify the compilation of partial stresses extreme values. Then the formula for checking the normal stresses in the cross-section of I-beam has the following form:

$$\sigma_{\max} = \left|\frac{M_y}{W_y}\right| + \left|\frac{M_z}{W_z}\right| + \left|\frac{M_\omega}{W_\omega}\right| \le f_y\,, \qquad (1)$$

where M_y, M_z – design bending moments relative to the *y*-axis and *z*-axis; according to the second-order theory are determined considering the rod angle of torsion [18] ($M_y^{II} = M_y^I + M_z^I \vartheta$; $M_z^{II} = M_z^I - M_y^I \vartheta$);

W_y, W_z – section moduli relative to the *y*-axis and *z* respectively;

M_ω – bimotent from transverse load or in the second-order theory from transverse load and beam curvature (M_ω^{II});

W_ω – warping section modulus of the beam;

f_y – yield strength.

To determine the beam angle of torsion ϑ and its derivatives, which are needed to find internal forces, the improved differential equation of the rod equilibrium [17], which considers rotational stiffness c_ϑ of fixing structures, can be used:

$$EI_\omega \vartheta^{IV}(x) - GI_t \vartheta''(x) + c_\vartheta \vartheta(x) = m(x), \text{ or} \tag{2}$$

$$EI_\omega \vartheta^{IV}(x) - GI_T \vartheta''(x) = m(x), \tag{3}$$

where E, G – modulus of elasticity and shear, respectively;

I_ω – warping constant of beam cross-section;

I_t – torsional constant of beam cross-section;

$m(x)$ – distributed torsion load;

I_T – increased torsional constant which considers the rotational stiffness c_ϑ, taking the sinusoidal shape of the torsion angle curve distribution along the beam length ($\vartheta'' \approx -\frac{\pi^2}{l^2}\vartheta$ or $\vartheta \approx -\frac{l^2}{\pi^2}\vartheta''$, then $I_T = I_t + \frac{c_\vartheta}{G}\frac{l^2}{\pi^2}$, similarly, the shear stiffness S can be considered).

For calculations of steel beams, both purlins and bars of cross-frames, a simplified method is sometimes used for the joint action of transverse bending and torsion, considering profiled flooring. Simplification in the second-order theory allows considering the increase of the beam rotational stiffness by introducing into the calculation of the conditional increased torsional constant I_T. But the formula for its determination is valid only with insignificant stiffness of flooring, which are reproduced in laboratory conditions. In vivo the stiffness of the roof is quite large, in addition, the bending in two planes and static uncertainty significantly increase the error.

The solution of equation (2), even with constant distributed torsion load, causes some difficulties. Therefore, the largest angle of torsion in the beam can be determined approximately, provided that the non-uniform distribution of the fictitious distributed torsion load from the pre-curvature $m_{x,0}(x)$ to the uniform equivalent action is replaced by the change in the curve of the pre-curvature for the sinusoid ($m(x) = m_q + m_{x,0}(x)$ replaced by $m = m_q + m_{x,0} \approx q_z e_y + q_y e_z + 0{,}85 q_z v_{0m} f_\vartheta$) according to the source [4], as follows:

$$\vartheta_m^I = \frac{5}{384}\frac{ml^4}{EI_\omega}\alpha_T^I \approx \frac{l^2}{EI_\omega}\left(\frac{M_{y0}e_y + M_{z0}e_z}{9{,}60} + \frac{M_{y0}v_{0m} f_\vartheta}{11{,}29}\right)\alpha_T^I, \tag{4}$$

where v_{0m} – the maximum pre-curvature, which depends on the beam span l;

M_{y0}, M_{z0} – conditional bending moments ($M_{y0} = q_z l^2/8$; $M_{z0} = q_y l^2/8$);

α_T^I – coefficient considering the elastic flexural-torsion constant ($\alpha_T^I = \left(1 + \frac{\varepsilon_T^2}{\pi^2}\right)^{-1}$; $\varepsilon_T = kl$; $k = \sqrt{\frac{GI_t}{EI_\omega}}$ or $k = \sqrt{\frac{GI_T}{EI_{\omega,D}}}$);

f_ϑ – coefficient which considers the distribution of bending moment along the length of the beam ($f_\vartheta = 1 + 0{,}566\psi(1+K)$, where ψ i K – the auxiliary coefficients for considering the support bending moments [4].

The torsion angle defined by formula (4) increases due to the influence of the second-order effects. This influence can be taken into consideration by the introduction of the magnification coefficient:

$$\vartheta_m^{II} = \vartheta_m^I \alpha_T^{II} \le 0{,}3, \tag{5}$$

where α_T^{II} – the magnification factor that considers elastic critical moment for LTB M_{cr}.

This coefficient can be determined by the expanded formula (6) [4] or the reduced formula (7) [5]

$$\alpha_T^{II} = \left(1 - \frac{M_{y0}}{M_{cr}}\frac{M_{y0} - k_p}{M_{cr} - k_p}\right)^{-1}; \tag{6}$$

$$\alpha_T^{II} = \left(1 - \frac{M_{y0}}{M_{cr}}\right)^{-1}, \tag{7}$$

where k_p – coefficient which considers the critical longitudinal force N_{cr} ($k_p = 0{,}81\zeta_0^2 N_{cr} z_p$, in this formula ζ_0 – coefficient which considers the distribution of the bending moment in the beam, see Table 6.2 [4]; z_p – the ordinate of the load application point, for the upper flange – the negative value).

The enlarged bimoment in the beam can be approximated defined similarly to the torsion angle as follows:

$$M_\omega^{II} = M_\omega^I \alpha_T^{II} = \left(EI_\omega \frac{\pi^2}{l^2}\vartheta_\omega^I\right)\alpha_T^{II} \approx \approx \left(\frac{M_{y0}e_y + M_{z0}e_z}{0{,}973} + \frac{M_{y0}v_{0m} f_\omega}{1{,}144}\right)\alpha_T^I \alpha_T^{II}, \tag{8}$$

where f_ω – coefficient considering the elastic flexural-torsion constant of the cross-section and the distribution of the bending moment along the beam length ($f_\omega = 1 + \frac{\varepsilon_T}{150} + 0{,}566\psi(1+K)$).

For a beam hingedly supported on the ends, which is loaded with a uniformly distributed load q_z, $f_\vartheta = 1$; $\zeta_0 = 1{,}12$; $f_\omega = 1 + \frac{\varepsilon_T}{150}$.

The marginal bearing capacity of the double symmetrical I-beam cross-sections for M_y, M_z and M_ω calculation in the plastic stage by the method of partial internal forces is given in Table. 7.10 [4] or in the article [21], but the maximum pre-curvature is assumed to be larger (25-50%).

The method by comparing the calculation results with finite element modeling in the Dlubal RSTAB 8.09 (FE-LTB additional module) was tested and the optimal shape of the formula for finding the α_T^{II} coefficient was found. Comparison of deformations, internal forces and normal stresses for one unrestrained rolled I-beam is given in Table 1.

Table 1: Comparison of calculation methods with numerical experiment

<table>
<tr><th>Cross-section</th><th>q_z, kN/m</th><th>l, m</th><th>v_{0m}, cm</th><th>Method</th><th>ϑ_m, mrad</th><th>M_z, kNcm</th><th>M_ω, kNcm^2</th><th>σ, kN/cm^2</th></tr>
<tr><td rowspan="5">40B1

steel grade S235</td><td rowspan="5">15</td><td rowspan="5">6</td><td rowspan="3">1,5 (0,5l/200),

LTB curve – c</td><td>FEA, by additional forces</td><td>121,8
100%</td><td>813,7
100%</td><td>18 872
100%</td><td>29,15
100%</td></tr>
<tr><td>SOT with formula (6)</td><td>132,3
108,6%</td><td>893,3
109,8%</td><td>20 178
106,9%</td><td>30,95
106,2%</td></tr>
<tr><td>SOT with formula (7)</td><td>186,1
152,8%</td><td>1255,9
154,3%</td><td>28 367
150,3%</td><td>40,10
137,6%</td></tr>
<tr><td colspan="2">EN 1993-1-1
($\chi_{LT,mod}$ = 0,384)</td><td>-</td><td>-</td><td>-</td><td>21,86
75,0%</td></tr>
<tr><td colspan="2">DBN V.2.6-198: 2014 (φ_b = 0,373)</td><td>-</td><td>-</td><td>-</td><td>22,52
77,3%</td></tr>
</table>

The comparison shows that the most appropriate numerical experiment is the technique for calculating the beam for the second-order theory with formula (6). Insignificant difference in these results is in the strength reserve, unlike normative methods.

The second-order theory is convincingly consistent with laboratory, full-scale and numerical experiments. Its approbation clearly shows that the insufficiently restrained structure at the elastic stage is very sensitive to the change in load and curvature, so when determining the load bearing capacity, the stiffness of the joints and the plastic work of the steel should be considered, if it is possible.

In the unrestrained channel beams, there is a regular torsion cross-section due to the load eccentric application. For accurate determination of maximum stresses, it is necessary to analyze the stress state of the beam cross-section in more detail. To calculate, as it is known, the stress at the most intense point of the cross-section should be checked. The largest absolute values of stress in the expanded formula are to be determined at two extreme points where like-sign stresses caused with bending in two planes occur. For the left lower point of the cross-section, all three components of the stress have the same sign, but the maximum normal stresses can operate in the right upper point of the cross-section since the flexural stress relative to the *z*-axis in it is much larger. The equation for determining normal stresses in general form is the following:

$$\sigma(y,z,\omega) = \frac{M_y}{I_y} z - \frac{M_z}{I_z} y + \frac{M_\omega}{I_\omega} \omega , \qquad (9)$$

where I_y, I_z – the second moments of cross-section area relative to the *y*-axis and *z* respectively;

z, y – coordinates of the cross-section considered the point where the stresses are determined relative to the gravity center;

ω – warping ordinate of the cross-section at the point where the stresses are determined.

In the second-order theory, the warping geometric properties during restraint ($I_{\omega,D}$; ω_D) are determined relative to the point of the lateral support, which is located on the beam rotation axis.

2.4 Determination of Geometric Properties Related to the Torsion of Rolled and Welded Beams

The geometrical properties associated with the torsion of non-closed profile beams include torsional constant, warping constant, the elastic flexural-torsional cross-section constant, the warping ordinate, the coordinate of the shear center, the parameter of monosymmetricity (Wagner coefficient), the stability parameter (auxiliary cross-section distance at monosymmetricity). The calculations using these geometric properties include: 1 – beams common and alternative (according to the second-order theory) calculation for general stability; 2 - calculation for the joint action of the transverse bend (in one or two planes) and torsion according to the thin-walled rods theory; 3 - calculation of beams with curvature in the plane of the least stiffness.

If the rods free torsion is considered separately, then during it tangential stresses occur in the element. For cross-sections consisting of several (n) narrow rectangles of length l_i and thickness t_i, the torsional constant is determined by the formula of Saint-Venan

$$I_t = \frac{\eta}{3} \sum_{i=1}^{n} \left(l_i t_i^3 \right) . \qquad (10)$$

The cross-section of the rolled I-beam is divided into rectangles rather identical (two complete flanges and a web). Considering the height of the cross-section *h* and the width of the cross-section *b* entirely, the angle between the flange and the web is taken twice, so this form of recording is irrelevant. Except dividing into two complete flanges and a web, the cross-section of the channel can be expanded to a complete web, which height is equal to the cross-section height, and the incomplete flanges adjacent to the web. If the flange thickness is greater than the web thickness, the first method gives the insignificant higher result of torsional constant calculating. But there is another rectangle partitioning method, which leads to the average result – at the midline. It seems to be the most reasonable in terms of the thin-walled rods theory, without considering corner R.

The alternative approach to determining torsional constant, taking into consideration corner R, obtained on the basis of the reference [22]. The increase in torsion constant due to corner R is performed according to the following scheme. The diameter of the largest circle, which can be inscribed at the joint, is determined and nondimensional coefficient *α*, obtained according to a graph or empirical formula, is introduced. There are various graphs and formulas for different cross-sections. The deduction on each free end is $0{,}105t_f^4$. When there are four ends, as it is in I-beam, it is necessary to make four deductions. When there are only two ends, as in a channel, two deductions are carried out (the above link source shows by mistake four deductions for the channels).

The influence degree of the corner R between the web and the flange on the correction factor η is determined, characterizing the type and complexity of the cross-section. This coefficient considers with simplifications the corner R presence between the cross-section divided into rectangles. So torsional constant I_t previously determined considering the constant empirical factor η = 1,29, for the channel cross-section, η = 1,11 is adopted.

To achieve this goal, the results of determining torsional constant for the selected I-beams with parallel flanges (according to GOST 26020-83) and the channels with tapered flanges (according to GOST 8240-89) were collected in the table 2. In columns 2, 4, 6, 9, 11, the increased torsional constant value is the first, considering the corner R between the web and the flange. In particular, the values of I_t in columns 2, 9 are calculated by the finite element method, 4 – by the Marc Villette formulas, being put into the special free program LTBeam, 6, 11 – according to the inscribed circle method. The SCAD Tonus, RAM Elements, Nastran (FEMAP) programs do not include corner R and give similar results. The Engineer Electronic Guide 2014 R3 implements the inscribed circle method with simplifications, which gives for I-beams rather overestimated results (up to 11% compared to FEA).

For rolled profiles, especially with a relatively large radius of corner R, the degree of proximity in expression (10) can be significant. A more precise estimate of the torsional constant correction for deductions at the open ends and its gain at the joints is justified and can be performed for I-beams in the program LTBeam, which showed the good convergence with the FEA, or with the inscribed circle method, shown for example, in [22]. The value of the correction factor η for rolled I-beams, based on the FEA results in the table, varies significantly between 1,23 and 1,60 (for the channels the effect is smaller – between 1,10 and 1,13) and requires analytical differentiated description.

Table 2: Determination of torsional constant I_t, см^4 and correction factor η for rolled I-beams and channels

№ I	Name of computer program or method						№ [	Name of computer program or method			
	Dlubal SHAPE-THIN 8.09	η	LTBeam 1.0.11	η	Inscribed circle method	η		Dlubal SHAPE-THIN 8.09	η	Inscribed circle method	η
1	2	3	4	5	6	7	8	9	10	11	12
10B1	1,143 / 0,851	1,34	1,179 / 0,858	1,37	1,157 / 0,882	1,31	5	0,846 / 0,753	1,12	0,909 / 0,834	**1,09**
12B1	0,979 / 0,743	1,32	1,009 / 0,748	1,35	0,996 / 0,762	1,31	6,5	1,048 / 0,949	***1,10***	1,113 / 1,039	1,07
14B1	1,311 / 1,054	1,24	1,349 / 1,060	1,27	1,338 / 1,085	***1,23***	8	1,304 / 1,177	1,11	1,372 / 1,279	1,07
16B1	1,878 / 1,394	1,35	1,916 / 1,401	1,37	1,934 / 1,432	1,35	10	1,650 / 1,491	1,11	1,714 / 1,604	1,07
18B1	2,617 / 2,043	1,28	2,669 / 2,053	1,30	2,673 / 2,101	1,27	12	2,122 / 1,905	1,11	2,179 / 2,030	1,07
20B1	6,768 / 4,996	1,35	6,884 / 5,024	1,37	6,916 / 5,165	1,34	14	2,671 / 2,395	1,12	2,719 / 2,540	1,07
23B1	8,236 / 6,364	1,29	8,374 / 6,395	1,31	8,416 / 6,587	1,28	16	3,305 / 2,957	1,12	3,339 / 3,126	1,07
26B1	8,073 / 6,316	1,28	8,277 / 6,347	1,30	8,279 / 6,480	1,28	16a	4,060 / 3,675	***1,10***	4,099 / 3,896	***1,05***
30B1	10,23 / 7,376	1,39	10,39 / 7,413	1,40	10,68 / 7,546	1,42	18	4,033 / 3,598	1,12	4,045 / 3,792	1,07
35B1	13,40 / 8,808	1,52	13,47 / 8,843	1,52	14,22 / 8,960	1,59	18a	4,908 / 4,429	1,11	4,923 / 4,682	***1,05***
40B1	21,47 / 13,46	**1,60**	21,50 / 13,52	**1,59**	22,95 / 13,70	**1,68**	20	4,862 / 4,325	1,12	4,844 / 4,547	1,07
45B1	32,34 / 22,19	1,46	32,45 / 22,28	1,46	33,67 / 22,63	1,49	22	6,157 / 5,466	**1,13**	6,098 / 5,742	1,06
50B1	45,41 / 33,42	1,36	45,69 / 33,21	1,38	46,40 / 33,67	1,38	24	7,833 / 6,950	**1,13**	7,710 / 7,288	1,06
55B1	69,36 / 49,82	1,39	69,84 / 50,03	1,40	71,55 / 50,83	1,41	27	9,804 / 8,713	**1,13**	9,653 / 9,124	1,06
60B1	101,5 / 76,96	1,32	102,5 / 77,29	1,33	103,6 / 78,79	1,31	30	12,36 / 10,92	**1,13**	12,17 /11,42	1,07
70B1	127,6 / 101,0	1,26	130,4 / 101,5	1,28	129,8 / 102,6	1,27	33	15,97 / 14,08	**1,13**	15,75 / 14,72	1,07
80B1	190,0 / 151,7	1,25	194,4 / 152,3	1,28	192,8 / 153,8	1,25	36	20,92 / 18,53	**1,13**	20,75 / 19,38	1,07
90B1	280,6 / 220,1	1,27	288,4 / 221,1	1,30	286,6 / 222,9	1,29	40	27,17 / 24,11	**1,13**	27,02 / 25,23	1,07
100B1	396,7 / 321,7	***1,23***	405,8 / 323,1	***1,26***	402,1 / 327,0	***1,23***	-	-	-	-	-

The greatest effect is achieved for medium height I-beams (35B1 – 45B1) and high channels (22 – 40). Corner R consideration in the place of flange attached to the web can significantly increase the value of the torsional constant. The following [22] formulas are recommended to be used to receive I_t considering corner R.

Due to the sufficiently small influence of corner R between web and flanges on the warping constant value, which is set out in [8], in the case of monosymmetric I-section, the formula for finding it relative to the shear center has a simplified form:

$$I_\omega = I_{zf1}\left[1-\frac{I_{zf1}}{I_z}\right]\left[h-\frac{t_{f1}}{2}-\frac{t_{f2}}{2}\right]^2; \qquad \left(I_{zf1}\neq 0\right), \tag{11}$$

Warping constant for the partially restrained I-beam relative to the rotation point is proposed to be determined by the chosen formula that corresponds to the numerical calculations results almost completely at an arbitrary shear stiffness *S* of the attached structures (for the rolled I-beam, the ratio of the lower and upper flange second moments of area $\frac{I_{zf2}}{I_{zf1}}=1$):

$$I_{\omega,D} = I_\omega\left(1+\left(\frac{S}{S_a}\right)^2\frac{I_{zf2}}{I_{zf1}}\right); \qquad \left(I_{zf1}\neq 0\right); \ \left(S\le S_a\right). \tag{12}$$

where S_a – the shear stiffness of the attached structures, is required for the restrained rotation axis adoption.

To find the warping constant of the channel cross-section, it is advisable to use the formula, but with the condition that the width and height of the cross-section are taken at the midline:

$$I_\omega = \frac{t_f b_s^3 h_s^2}{12}\cdot\frac{3+2\eta\psi}{6+\eta\psi}, \tag{13}$$

where $\eta = h_s/b_s$; $\psi = t_w/t_f$ – the ratio of the cross-section sizes (Fig. 2).

It is known that the normal torsion stresses are distributed in the beam cross-section proportional to the warping ordinate, which is equal to the double area, restricted by the contour of the section and two radius-vectors, made from the shear center (point *S* in Fig. 2) in the cross-section initial and considered point of the contour (midline). For I-beam symmetrical cross-section, shear center coincides with the gravity center; for the channel cross-section, it has the coordinate *e* relative to the web center. However, when fixing as the shear center, the variable point *D* serves, which is in the cross-section axis of rotation.

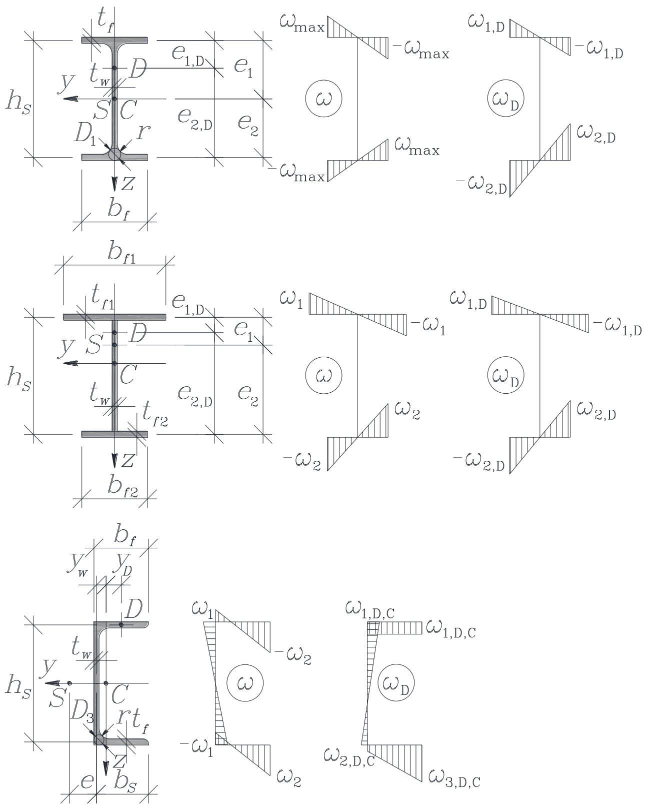

Fig. 2: Torsion geometric properties determination; diagrams of warping ordinates of the cross-section for unrestrained and restrained rolled and welded beams

For I-beam, the maximum warping ordinate of the cross-section ω_{max} (Fig. 2) can be determined by the simplified formula:

$$\omega_{max} = 0,25 b_f h_s, \tag{14}$$

where b_f – flange width;

h_s – distance between flanges centers.

For a monosymmetric I-beam, the warping ordinates of the cross-section ω_1 and ω_2 in unrestrained beams, as well as the coordinates $\omega_{1,D}$ and $\omega_{2,D}$ (Fig. 2) relative to the point located on the axis of rotation during restraint, are determined by the formulas:

$$\omega_1 = 0,5b_{f1}e_1;\ \omega_2 = 0,5b_{f2}e_2; \quad (15)$$

$$\omega_{1,D} = 0,5b_{f1}e_{1,D};\ \omega_{2,D} = 0,5b_{f2}e_{2,D}, \quad (16)$$

where b_{f1} – upper flange width;

b_{f2} – lower flange width;

e_1 – distance from the shear center to the upper flange center;

e_2 – distance from the shear center to the lower flange center;

$e_{1,D}$ – distance from the point of rotation to the upper flange center;

$e_{2,D}$ – distance from the point of rotation to the lower flange center.

The position of the rotation axis relative to the shear center at an arbitrary shear stiffness S of the attached structures is established considering that the distance between them at zero stiffness is zero, and when the required stiffness S_a is achieved, the restrained rotation axis of the beam passes through the center of the upper flange where there is an adjacency lateral support. Then the distances e_1 and e_2 (for the rolled I-beam, $e_1 = e_2 = 0,5h_s$), as well as the distances $e_{1,D}$ and $e_{2,D}$, are:

$$e_1 = \frac{I_{zf2}}{I_z}h_s;\ e_2 = \frac{I_{zf1}}{I_z}h_s; \quad (17)$$

$$e_{1,D} = e_1 - \frac{S}{S_a}e_1;\ e_{2,D} = e_2 + \frac{S}{S_a}e_1. \quad (18)$$

For a channel, the warping ordinates ω_1 and ω_2 (Fig. 2) without considering the restraint and ordinates $\omega_{1,D,C}$, $\omega_{2,D,C}$ and $\omega_{3,D,C}$ (they consist of their own ordinates relative to the rotation point $\omega_{1,D}$, $\omega_{2,D}$ and $\omega_{3,D}$ and the ordinate of the rotation point relative to the center of gravity $\omega_{D,C}$) in the case of the restrained rotation axis passing through the center of the upper flange, are determined by the simplified formulas:

$$\omega_1 = 0,5h_s e;\ \omega_2 = 0,5h_s\left(b_s - e\right); \quad (19)$$

$$\omega_{1,D,C} = \omega_{1,D} + \omega_{D,C} = -h_s(y_w + 0,5y_D); \quad (20)$$

$$\omega_{2,D,C} = \omega_{2,D} + \omega_{D,C} = 0,5h_s y_D; \quad (21)$$

$$\omega_{3,D,C} = \omega_{3,D} + \omega_{D,C} = h_s(y_w + 1,5y_D + 0,5b_f), \quad (22)$$

where e – distance from the shear center to the web center;

b_s – flange width from the free end to the web center;

y_w – distance along the y-axis from the center of gravity C to the web center;

y_D – distance along the y-axis from the point of rotation D to the center of gravity C.

The distance from the shear center to the web center is logical to determine by the geometric properties determination according to the strength of materials rules:

$$e = \frac{b_s}{2 + \dfrac{h_s t_w}{3b_s t_f}}. \quad (23)$$

Then warping constant for the restrained channel beam relative to the rotation point is proposed to be determined by the derived formula that corresponds to the numerical calculations results almost completely at a sufficient shear stiffness $S \geq S_a$ of the attached structures:

$$I_{\omega,D} = b_s t_f \omega_{1,D,C}^2 + \frac{1}{3}h_s t_w\left(\omega_{1,D,C}^2 + \omega_{1,D,C}\omega_{2,D,C} + \omega_{2,D,C}^2\right) + \frac{1}{3}b_s t_f\left(\omega_{2,D,C}^2 + \omega_{2,D,C}\omega_{3,D,C} + \omega_{3,D,C}^2\right). \quad (24)$$

The Wagner coefficient for vertical asymmetry and the monosymmetric parameter (Wagner negative coefficient) can be accurately determined considering the corner R (LTBeam program) or without corner R (for example, the program ConSteel) through a specific stability parameter and coordinate of the shear center S relative to the gravity center (centroid) C.

2.5 A Modified Method for Calculating Roof Purlins

It should be noted that for channel purlins according to [8] torsion calculation reduces the calculated normal stresses by an average of 15% compared to bending in two planes. And the forces arising from the eccentricity of attaching the beam to the bolts on the supports, theoretically, can reduce the stresses in the dangerous cross-section more than twice (for inclined purlins fixed by the web). In fact, this decrease will be lower due to the looseness of bolted joints, but its impact should be considered. Therefore, the channel is considered to be the optimal cross-sectional shape for the sloping roof. However, in a real restrained structure, the profiled flooring increases the purlin rotational stiffness, so the effect is different. In addition, it is known that with sufficient shear stiffness it is assumed that the compressed flange is completely fixed and the transverse displacements cannot occur; and the axis of rotation which is called restrained or fixed passes along the beam top. For a channel, the axis of rotation then is located at the center of the upper flange where loads are applied that do not have eccentricities relative to this point. Therefore, warping stresses from a transverse load are not practically formed. But telling economy can be achieved by reducing the effect on the stresses of the load slope component. Normal stresses in the restrained beam at the calculation of the overall stability by bending in two main planes are proposed to be determined using the formula (9) with specification. The bending moment slope component decreases by multiplier:

$$C_r = \frac{v_{oc,m}}{v_q}. \quad (25)$$

where C_r – a coefficient equal to the ratio of the upper flange maximum displacement $v_{oc,m}$ of the beam restrained by profiled flooring (it is possible to find in [17]) to the beam maximum curvature v_q from the load slope component; for the beam hinged on ends $v_q = \frac{5}{384}\frac{q_y l^4}{EI_z}$).

With continuous side-restraint with a certain shear stiffness, the upper flange is displaced under the external and equivalent loads. The deformation of the upper flange arises due to the flexibility of the attachment. Considering the second-order theory and the compressed rod changed model (with considering the bending moment distribution along the beam length) to be the basis, the simplified equation has been obtained to determine the upper flange maximum displacement of the beam restrained by profiled flooring, which leads to a slight results overstatement accounting for the strength reserve, but is easy to apply:

$$v_{oc,m} = \frac{\alpha_{II}(M_z + M_e)}{S} = \frac{M_z + N_c v_{0,m} n}{S - N_c n} \approx \frac{M_z + N_c \bar{v}_{0,m} n}{S}, \quad (26)$$

where $\alpha_{II} = \left(1 - \frac{N_c n}{S}\right)^{-1}$ – magnifying factor, which considers the flexibility of restricted structures;

$M_e = N_c v_{0,m} n$ – bending moment from equivalent load;

$N_c = \frac{C_d M_y}{h_s}$ – longitudinal compressive force in the upper flange with considering the bending moment distribution along the beam length (for a uniformly distributed load by the change in the curve of the pre-curvature for the square parabola C_d = 0,833 according to own calculations or by the change in the curve of the pre-curvature for the sinusoid C_d = 0,885 according to the source [17]);

$v_{0,m}$ – maximum beam pre-curvature, which is determined depending on the curvature type, cross-section and span (e_0 in accordance with the notation EN 1993-1-1);

n – the number of restrained beams; the two marginal beams are taken as one since they have only half the cargo area;

S – shear stiffness of restraining structures (profiled flooring or profiled flooring and discrete joints).

It should be noted that the expression (26) does not consider the component of the equivalent load arising from the torsion of the channel beam applied to the eccentricity of the main load and other factors, as it does not contribute increasing the structure reliability due to unloading. Moreover, it complicates the calculation. Therefore, it was decided to use the formula EN 1993-1-1.

The flexibility of the upper flange can be considered approximately through the acceptance of the increased beam pre-curvature, which includes the deformation of the upper flange under load ($\bar{v}_{0,m} = v_{0,m} + v_{oc,m}$). The increased beam pre-curvature considers the effect of the transverse displacements of the upper flange flexible attachment, caused by the external and equivalent load action. In this case, the maximum displacement of the upper flange fixed by profiled flooring at the small angles of torsion should not exceed the value of beam curvature from the external load. Since beam upper flange maximum displacement and the equivalent load depend on each other, the increased pre-curvature must be determined in an iterative way.

Bimoment from pre-curvature by the change in the curve of the pre-curvature for the sinusoid can be determined by formula:

$$M_\omega = -EI_{\omega,D}\vartheta''(x), \quad (27)$$

where $\vartheta''(x)$ – the second derivative of the torsion angle function in the form of a expression with two or more parameters, which can be determined by the matrix method [17], subject to replacement I_ω by $I_{\omega,D}/2$.

Consideration of bimoment from pre-curvature by the change in the curve of the pre-curvature for the square parabola is proposed to be carried out in accordance with the thin-walled rods theory for a uniformly distributed load according to the specified formula:

$$M_\omega = \frac{q_z \bar{v}_{0,m} \mu_q}{k^2}, \quad (28)$$

where μ_q – the coefficient, which depends on the flexural-torsional constant of the cross-section k and the beam span l; ($\mu_q = 1 - \frac{\tanh(kl/2)}{kl/2}\frac{\tanh(kl/4)}{kl/4}$ or in Fig. 3).

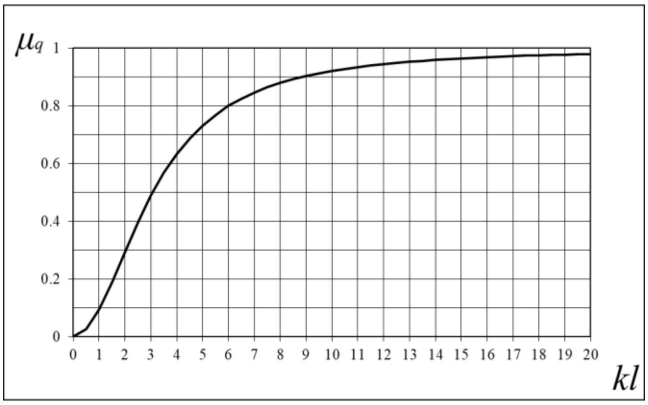

Fig. 3: Graph for determining the coefficient μ_q

The actual operation of the channel purlin in the structure of the sloping roof, despite its prevalence, is often misinterpreted due to the description complexity, which leads to analytical errors in the calculation process. It is especially correct for determining the bimoment, which depends on the function of the rod torsion angle. The distribution of these deformations along the element length has been analyzed. It is important to note that in actual practice, the calculated bimoment depends not only on the load, its eccentricity, the cross-section elastic flexural-torsional constant and beam span, but also on the stiffness of the structures attached to the beam.

Even with the attachment of profiled flooring in every other rib, its shear stiffness often reaches sufficient value for the adoption of beam rotation restrained axis on the reduced required shear stiffness criterion. Modeling by the finite element method showed that in this case, the bending moment in the plane of the least stiffness significantly decreases and its effect on the general stress-strain state practically reduces to zero. The function of the rod torsion angle is often described in the literature with the help of a monomial equation using the half-wave of the sinusoid, which usually results in more or less precise results. Since the limits of use are rarely determined clearly, there may be negative deviations. Thus, the presence of profiled flooring with significant rotational stiffness and the load slope component causes a tangible distortion of the torsion angle curve distribution along the beam length. This, in turn, leads to noticeable changes in the bimoment value.

3. Conclusion

Considering the factors mentioned in the article that characterize the features of the steel beams behavior as the part of roofing at complex resistance, it is possible to determine the values of normal and warping stresses affecting the structure overall stress-strain state and the design ratio more precisely. When calculating and investigating, it is suggested to pay attention to the following factors:

1) the rod torsion angle substantially affects the value of the calculated bending moments in two planes, therefore, in the absence of the formula for determining the total stresses of the reduction factor for LTB, which is deducted for the system deformed state, the cross-section rotation phenomenon should be considered;

2) the consideration of attached structures stiffness in determining the torsion geometric properties of beam cross-section reflects the beam actual work in decking more accurately;

3) considering the corner R in the place of flange and web joint allows to increase torsional constant value in the rolled profiles significantly;

4) in the presence of lateral restraint and the load slope component, the effect of the latter on the stresses is significantly reduced by decreasing the deformations in the plane of less stiffness (beam curvature);

5) when taking the restrained axis of rotation, warping stresses in beams of sloping roof from a transverse load are not practically formed;
6) the reason for the emergence of warping stresses can be not only the transverse load, but also the presence of geometric imperfection, namely the pre-curvature, which can be considered by increasing the uniformly distributed torsion load, which increases the bimoment, or by the determination of additional stresses;
7) considering the existing reserves of steel plastic work can be carried out by calculating the beam bearing capacity in the plastic stage by the partial internal forces under the action of moments and bimoment method and accepting a greater maximum pre-curvature;
8) the forces arising from the eccentricity of beam attaching to the bolts on the supports, can significantly reduce the stresses in the dangerous cross-section, despite the bolted joints looseness;
9) the distribution angle of torsion along the beam length, even with hinged support at the ends and applying even uniformly distributed torsion load is not recommended to accept sinusoidal in the case of roof significant stiffness;
10) when determining the elastic critical moment for LTB, it is expedient to consider the rotational or rotational and shear stiffness of the structures, which restrain the beam compressed flange, prone to stability loss.

Acknowledgement

The work was carried out at Poltava National Technical Yuri Kondratyuk University, and its main results were implemented within the framework of the state budget scientific theme: "New universal resource-saving structural solutions for long span buildings and structures decking and energy-saving technology of their construction" (state registration number 0117U003907).

References

[1] Balázs I. and Melcher J., Stability of Thin-Walled Beams with Lateral Continuous Restraint, Transactions of the VŠB–Technical University of Ostrava, Civil Engineering Series, 15(1), (2015), pp.1-10. https://doi.org/10.1515/tvsb-2015-0001
[2] Put B.M., Pi Y.L. and Trahair N.S., Bending and torsion of cold-formed channel beams, Journal of Structural Engineering, 125(5), (1999), pp.540-546. https://doi.org/10.1061/(ASCE)0733-9445(1999)125:5(540)
[3] Pavlenko A.D., Rybakov V.A., Pikht A.V., Mikhailov E.S., Non-uniform torsion of thin-walled open-section multi-span beams, Inzhenerno-stroitel'nyy zhurnal, №7(67), (2016), pp:55-69, https://doi.org/10.5862/MCE.67.6
[4] Kindmann R., Stahlbau, Teil 2: Stabilität und Theorie II. Ordnung. 4. Auflage, Berlin: Ernst & Sohn, (2008), 429 p, https://doi.org/10.1002/9783433600030
[5] Kuhlmann U., Stahlbau-Kalender 2009: Schwerpunkt – Stabilität, Berlin: Ernst & Sohn, (2009), 1032 p.
[6] Wagenknecht G. Stahlbau-Praxis nach Eurocode 3: Band 1 Tragwerksplanung, Grundlagen, Berlin: Beuth Verlag GmbH, (2011), 396 p.
[7] Vlasov V.Z., Tonkostennyye uprugiye sterzhni, M.: Gosizdat, Fizmatgiz – matematicheskoy literatury, (1959), 568 p.
[8] Bychkov D.V., Stroitel'naya mekhanika sterzhnevykh tonkostennykh konstruktsiy, M.: Gosstroyizdat, (1962), 476 p.
[9] Tusnin A.R., Prokich M., Rabota simmetrichnykh dvutavrovykh secheniy pri razvitii plasticheskikh deformatsiy i deystvii izgibayushchego momenta i bimomenta, Inzhenerno-stroitel'nyy zhurnal, №5(49), (2014), pp:44-53, https://doi.org/10.5862/MCE.49.5
[10] Tusnin A.R., Prokich M., Eksperimental'nyye issledovaniya raboty balok dvutavrovogo secheniya pri deystvii izgiba i krucheniya, Inzhenerno-stroitel'nyy zhurnal, №1, (2015), pp:24-31, https://doi.org/10.5862/MCE.53.3
[11] Selyantsev I.M., Eksperimental'naya otsenka vliyaniya deformatsii kontura poperechnogo secheniya na rabotu tonkostennykh sterzhney otkrytogo profilya, Nauchno-tekhnicheskiy vestnik Povolzh'ya, (6), (2012), pp:370-373.
[12] Kindmann R. and Kraus M., Steel structures: Design using FEM, John Wiley & Sons, (2011), pp:168-216, https://doi.org/10.1002/9783433600771.ch5
[13] Pilkey W.D., Analysis and design of elastic beams: Computational methods, John Wiley & Sons, (2002), pp:312-368, https://doi.org/10.1002/9780470172667.ch7
[14] Trahair N.S., Bradford M.A., Nethercot D.A. and Gardner L., The behaviour and design of steel structures to EC3, CRC Press, (2007), pp:227-294.
[15] Martin L. and Purkiss J., Structural Design of Steelwork to EN 1993 and EN 1994, CRC Press, (2007), pp:35-174.
[16] Galambos T.V. and Surovek A.E., Structural stability of steel: concepts and applications for structural engineers, John Wiley & Sons, (2008), pp:236-289, https://doi.org/10.1002/9780470261316.ch6
[17] Krahwinkel M., Zur Beanspruchung stabilisierender Konstruktionen im Stahlbau, Fortschritt-Berichte VDI, Reihe 4 Bauingenieurwesen, Nr. 166, Düsseldorf: VDI-Verlag, (2001), 182 p.
[18] Hudz S.A., Nesucha zdatnistʹ stalevykh dvotavrovykh balok, shcho ekspluatuyutʹsya z nedoskonalostyamy u vyhlyadi pochatkovykh vykryvlenʹ u ploshchyni naymenshoyi zhorstkosti, Visnyk Odesʹkoyi derzhavnoyi akademiyi budivnytstva ta arkhitektury, Vyp. № 61, Odesa: Zovnishreklamservis, (2016), pp:95-101.
[19] Hudz S.A., Hasenko A.V., Vplyv zhorstkosti pryyednanykh konstruktsiy na stiykistʹ balok, Zb. nauk. pratsʹ: Shlyakhy pidvyshchennya efektyvnosti budivnytstva v umovakh formuvannya rynkovykh vidnosyn, Vyp. 35, Tekhnichnyy, K.: KNUBA, (2018), pp:114-123.
[20] G. Gasii, O. Hasii, and O. Zabolotskyi, Estimate of technical and economic benefits of a new space composite structure. MATEC Web of Conferences, Vol. 116, (2017), pp. 02014, https://doi.org/10.1051/matecconf/201711602014
[21] Kindmann R. and Ludwig C., Plastische Tragfähigkeit von gewalzten und geschweißten I-Querschnitten, Stahlbau, 83(12), (2014), pp:890-904, https://doi.org/10.1002/stab.201410223
[22] Tata Steel, Steel building design: design data, The Steel Construction Institute and The British Constructional Steelwork Association Limited, (2013), 690 p.
[23] Storozhenko, L., Butsky, V., Taranovsky, O. Stability of Compressed Steel Concrete Composite Tubular Columns with Centrifuged Cores // Journal of constructional steel research; 46, 1/3; 484; Second World Conference on Steel in Construction ; 1998.
[24] Piskunov, V.G., Gorik, A.. & Cherednikov, V.N. Mechanics of Composite Materials (2000) 36: 445. https://doi.org/10.1023/A:1006798314569
[25] Kochkarev D. Calculation methodology of reinforced concrete elements based on estimated resistance of reinforced concrete / D. Kochkarev, T. Galinska // Matec Web of Conferences 116, 02020 (2017), Materials science, engineering and chemistry, Transbud–2017, Kharkiv, Ukraine, April 19–21, 2017. https://doi.org/10.1051/matecconf/201711602020